Water Droplet Avalanches

Britton Plourde, Franco Nori, and Michael Bretz
Department of Physics, The University of Michigan, Ann Arbor, Michigan 48109-1120
(Received 8 July 1993)

We analyze the statistics of water droplet avalanches in a continuously driven system. Distributions are obtained for avalanche size, lifetime, and time between successive avalanches, along with power spectra and return maps. For low flow rates and different water viscosities, we observe a power-law scaling in the size and lifetime distributions of water droplet avalanches, indicating that a state with no characteristic time and length scales was reached. Higher flow rates resulted in an exponential behavior with characteristic scales.

PACS numbers: 64.60.Ht, 05.40.+j, 05.70.Ln

The deposition, growth, coalescence, and motion of fluid droplets is a subject of enormous interest to many disciplines in science and engineering [1]. Examples of fluid transport that have recently attracted renewed interest include models of river formation [2] and the coverage area fluctuations of periodically pulsed droplet deposition [3]. Also, studies of a *single* dripping faucet have found a rich dynamics, including period doubling, as a function of the water supply flow rate [4]. Lightning discharges and other forms of electrical breakdown [5], aperiodic x-ray sources [6], plasma turbulence, mechanical vibrations, and electronic circuits [7] can sometimes be characterized in terms of spatially extended "dripping" models. The literature on water droplet dynamics is vast, and we do not attempt a review. The interested reader is referred to our references and papers cited therein. Here, we present an investigation of the dynamics of avalanches in continuously driven water droplet systems.

Recently, the notion of self-organized criticality has been proposed [8] to account for the behavior of certain driven dissipative dynamical systems which exhibit long-range spatial and temporal correlations. Upon reaching the critical attractor, avalanches are produced with lifetime and size distributions which decay as power laws. Many previous avalanche studies have examined the onset of collective transport in a wide variety of systems in which noncoalescing interacting elements (e.g., sand grains, vortices) can be identified. Examples include granular materials [9] and vortices in superconductors [10]. Our study is one of the few systematic investigations of collective dynamics in a system with coalescing moving elements (i.e., a fluid). An avalanche on a tilted sprayed surface occurs when a droplet grows in size and eventually reaches a critical mass, at which time it runs down the surface, triggering other stationary droplets in its path, thus creating a chain reaction [11]. Here, we examine the power spectra and distributions of water droplet avalanche sizes, lifetimes, and delay times between successive events in an analogous manner to previous studies of avalanches.

The experimental apparatus is illustrated in Fig. 1(a). Distilled water was sprayed through a flow-regulated forced-air mister into a clean, clear plastic dome. The water spray was collected inside the dome, producing streams which ran down and eventually dripped off the rim. The droplets then impacted on, and immediately ran off of a light slanted ring, which was suspended by a piezo film detection system.

Figure 1(b) displays the anatomy of one of the three piezo film detectors. A drop of water falling on the ring stretched the film longitudinally, thus producing a measurable voltage from which we determined the time stamp and size of the water droplet avalanches. Each piezo strip transducer consisted of a thin Mylar film of double-coated piezoelectric material, which was hung

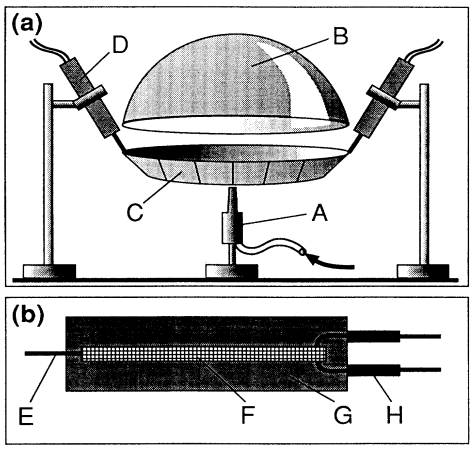

FIG. 1. (a) Schematic diagram of the experimental apparatus: distilled water is sprayed through the spray mister (A) into the transparent plastic (plexiglass) dome (B). Streams then run down the dome, drop onto the slanted annular impact ring (C), and immediately drop off the inner rim of the ring. Their impulse onto the ring produces signals from the three piezo film detectors (D), mounted at 120° intervals, one of which is not shown for clarity. (b) Detailed diagram of a piezo film detector: upon a droplet impulse, the suspension wire (E) stretches the piezo film strip (F), enclosed in a copper shield (G), sending an electric signal to the computer through coaxial cables (H).

0031-9007/93/71(17)/2749(4)$06.00

within a copper housing. Each of the three signals was sharpened by an RC filter, passed through an amplifier circuit, and was digitized using a Data Translation 2805 converter board. Data were acquired at a sampling rate of 4 kHz using a double-buffered direct memory access analog-to-digital conversion technique which allowed for a continuous flow of data at 1.33 kHz per channel.

Each droplet impacting the ring produced direct signal responses followed by post-impact (or aftershock) damping vibration signals in all three detectors. A program was written in C^{++} to compare the detector signals with pipette calibrated impulses, to test a cutoff value for screening out aftershocks, to sum the signals, and to output a time stamp and relative size of each event. Calculation of the relative event size was possible because the total detector signal produced by one fixed size droplet was essentially independent of angular position around the ring.

Because this detection system could discern droplets separated in time by only a few milliseconds, it was necessary to define a clustering time, $T_{\rm cl}$, for droplets that were considered to be causally connected to each other, and not independently triggered. The individual droplet signals (with a duration on the order of 0.5 msec) separated by less than $T_{\rm cl}$ were considered to be part of the same avalanche (i.e., an event composed of one or more individual droplets), with a total size equal to the sum of the sizes of the constituent individual droplets. The time stamp was assigned as that of the initial droplet time. The value of $T_{\rm cl}$ could be easily altered in the analysis program, allowing us to test many different values on the same raw data set and to view the effects. For $T_{\rm cl} \leq 5$ msec, droplets which were observed to be correlated were artificially subdivided into separate events. For $T_{\rm cl} > 7$ msec, a visual observation of the output indicated that the evaluation program summed many small uncorrelated events, lumping them together as larger avalanches. Therefore, we have chosen $T_{\rm cl} = 6$ msec. This evaluation method also made it straightforward to define an avalanche lifetime, τ, as the time from the initial to the final droplet in a given avalanche, and also a delay time, Δt, between avalanches.

The system produced many water streams which ran down the surface, often resulting in water accumulations around the rim of the dome. Drops then fell off the rim and impacted the ring when they acquired the critical mass needed to overcome surface tension effects of the edge, or when a fast moving droplet hit an accumulation and triggered an avalanche. Since the detection method could only monitor avalanches that actually fell off the dome, it was decided to minimize this accumulation problem by attaching many 1 cm long vertical copper wires along the rim, thus preventing rim droplets from coalescing and lingering. In early stages of this experiment, mechanical vibrations were a significant problem. The dome base was therefore fit with a thick brass outer sleeve and tightly wedged in a mechanically rigid frame, thereby removing vibrations.

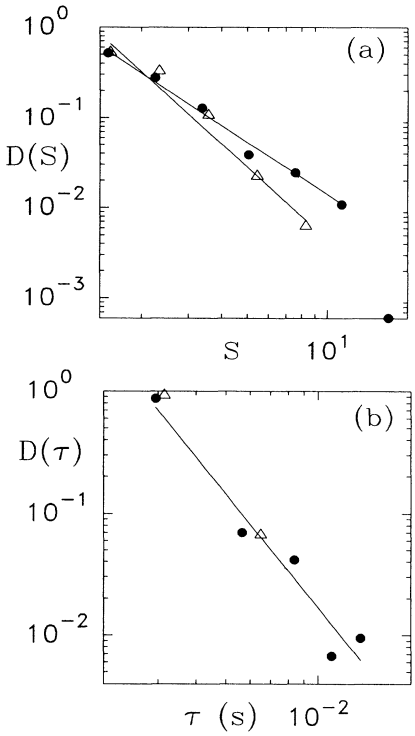

FIG. 2. Distributions of water droplet avalanche sizes, $D(S)$, (a) and lifetimes, $D(\tau)$, (b) for two 3.5 h runs with a flow rate of 8 cm^3/min at two different viscosities (temperatures): low viscosity ($\sim$ 22 °C) ($\triangle$) producing 2569 avalanches; and high viscosity ($\sim$ 1 °C) ($\bullet$) producing 2961 avalanches. In this paper, $\triangle$ always correspond to high T data, while ($\bullet$) represent low T data. S is dimensionless since it is obtained as a ratio of voltages.

In order to examine the effects of increasing the water viscosity, the water temperature was lowered. By chilling water from room temperature to near freezing, the water viscosity approximately doubles. At 25 °C the viscosity of water is 0.89 cP, while at 1 °C the viscosity is 1.73 cP. This method of varying the viscosity appeared to be simpler and more controlled than using a fluid other than water. Cooling was accomplished by adding chilling elements to the dome, spray nozzle, and water reservoir.

Data runs were taken at many different flow rates, for both high and low temperatures. The results shown here represent two data runs of 3.5 hours each with a low flow rate (8 cm^3/min): one at about 22 °C and one near 1 °C (hereafter denoted as "high T" and "low T," respectively). Figure 2 contains the distributions of avalanche sizes, $D(S)$, and lifetimes, $D(\tau)$. Figure 3 shows the corresponding distributions of time delays between consecutive avalanches (sometimes called waiting times), $D(\Delta t)$. The plots have been scaled so that the sum of the probabilities for each data set is equal to 1. All of our data were examined on semi-log and log-log plots, with both linearly and logarithmically binned histograms. The lat-

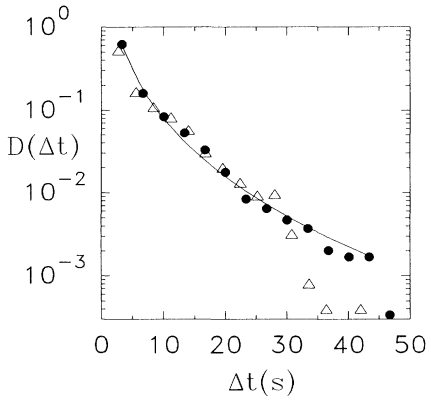

FIG. 3. Distributions of delay times between successive avalanches, $D(\Delta t)$, for the same data described in Fig. 2.

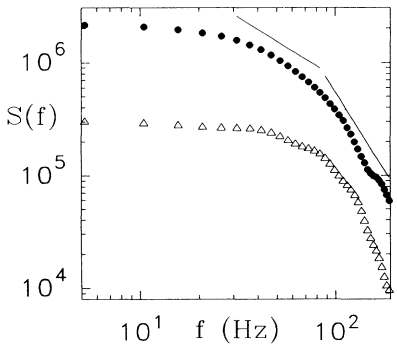

FIG. 4. Power spectrum versus frequency (in hertz) for the same data shown in Fig. 2. Straight lines denote slopes of -1 and -2.7. For clarity, data has not been normalized.

ter have bin heights which were normalized by their corresponding bin widths. These alternate plotting and binning methods helped us to discern between exponential, power-law, or other types of decays.

The low flow rate size distributions, Fig. 2(a), exhibit a power-law behavior, as shown by the linear fits: $D(S) \sim S^{-a}$, with $a = 2.66$ (1.93) for low (high) viscosity. The high flow rate size distributions (not shown) exhibit an exponential behavior: $D(S) \sim \exp\{-(S/S_0)\}$, with $S_0 \sim 1.2$, consistent with single droplets. $D(\tau)$ for the high T data, Fig. 2(b), extended over a somewhat narrow range of τ due to the low water viscosity. By lowering the temperature, and thereby increasing the "cohesive strength" between the droplets (i.e., water viscosity), $D(\tau)$ extends over a longer τ range. The linear fit in Fig. 2(b) indicates a power-law behavior over about a decade: $D(\tau) \sim \tau^{-3.10}$. The high flow rate lifetime distributions (not shown) exhibit an exponential behavior: $D(\tau) \sim \exp\{-(\tau/\tau_0)\}$, with $\tau_0 \sim 2$ msec (short avalanches). Low water flow rates are analogous to slowly driving the system towards the threshold of instability, as in other avalanche studies [9,10]. High flow rates drive the system very rapidly, preventing a broad distribution of relaxation rates, resulting in exponential distributions of sizes and lifetimes.

At low T and low flow rates, there were several, somewhat periodic, large events which were significantly larger than the largest events in the high T data sets. These large events correspond to avalanches which span a significant portion of the dome surface and sweep up many stationary droplets in their paths, thus acting like "system-resetting" events. After the occurrence of any one of these large events, the behavior was characterized by only small and medium size avalanches for a long period of time. Eventually the system collected enough stationary droplets to have the potential for another system-resetting avalanche. This behavior is reminiscent of the relaxation oscillations in sandpiles [9], where every "period" exhibits precursor avalanches leading up to a large system-spanning slide, which resets and relaxes the system, followed by a series of small aftershocks. The large water avalanches occurred because the higher viscosity obtained at low T provided more "cohesion" between the droplets, allowing them to accrete into much larger clusters on the surface before avalanching.

The distributions, $D(\Delta t)$, of delay time intervals between successive events shown in Fig. 3 exhibit a stretched exponential behavior: $D(\Delta t) \sim \exp\{-(\Delta t/\Delta t_0)^{1/4}\}$, where $\Delta t_0 = 2.8$ msec (for the low T data shown). The $D(\Delta t)$ for the low T, high viscosity data has a higher Δt tail than the corresponding tail for the high T, low viscosity data. At any given T, we found that increasing the flow rate caused the range of the Δt tails to be compressed. This is consistent with mass conservation: The more quickly water is sprayed into the system, the more closely spaced the resulting avalanches will be. The small exponent in the fit of the high viscosity data suggests that correlations among droplet avalanches are significant.

Figure 4 shows the power spectra obtained by squaring the Fourier transform of the avalanche time trace. These power spectra, with three different "regions," are similar to those published in some previous theoretical avalanche studies [12]. At higher viscosities (low T), one might identify three approximate power-law regimes: a high-frequency regime ($f \geq 90$ Hz) with a slope of about -2.7, corresponding to observation times smaller than our largest lifetime avalanche; an intermediate regime ($30 \leq f < 90$ Hz) with a slope of the order of -1, corresponding to times larger than the maximum duration (lifetime) of individual avalanches (~ 13 msec), and denoted [12] as the regime of interacting avalanches; and a low-frequency regime ($f < 30$ Hz, for low T) with an approximately flat slope, characteristic of white noise, and corresponding to uncorrelated events widely separated in time. For the low viscosity data (high T), the middle-frequency regime is small, while the (low-frequency) white noise region extends significantly (up to $f \sim 40$ Hz). This demonstrates that for lower viscosities, the avalanches are more weakly correlated than the higher viscosity events. Of course, and as discussed

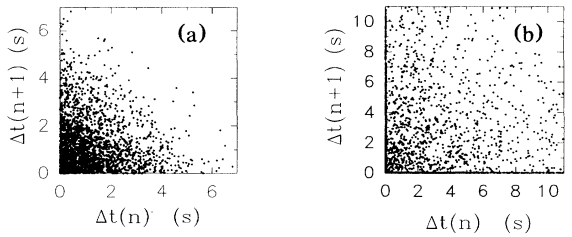

FIG. 5. Return maps, Δt_{n+1} versus Δt_n, for high viscosity data (low T) at two different flow rates: (a) 17 cm^3/min, and (b) 8 cm^3/min. A steep decay in $D(\Delta t)$ for high flow rates produces a dense cluster of data around a triangular region near the origin. A slowly decaying $D(\Delta t)$ for low flow rates produces a much more diffuse distribution of data.

by Weissman, Jensen, and others [13], any occurrence of a $1/f$ region by itself should not be considered definite evidence in support of self-organized criticality.

Our distributions demonstrate that avalanches with many different sizes and time delays occur. To examine if there are significant correlations between consecutive avalanches, we have studied the Δt return maps. Figure 5 shows Δt_{n+1} versus Δt_n for the high viscosity (low T) data set for two flow rates: (a) 17 cm^3/min, and (b) 8 cm^3/min. In previous dripping faucet chaos experiments [4], this graph produced "periodic" islands with interesting fractal shapes and some purely stochastic distributions, illustrating period-doubling behavior as a function of the faucet flow rate. However, in our return map, there is a fundamentally different behavior. Instead of periodic islands, there is a high concentration along the axes and a dense triangular region at the origin. For high flow rates, event pairs with a large time delay are usually followed by another avalanche a short time later. Conversely, event pairs with smaller time delays are followed by an avalanche with an increasingly larger range of time delay possibilities. However, for low flow rates, the return map is more uniformly distributed due to the broader distribution of delay times. The observed behavior is the result of the many degrees of freedom involved in the dynamics, because this system can be thought of as a large array of interacting dripping faucets.

Very large avalanches [e.g., $D(S = 17)$ in Fig. 2(a)] are rare, and thus are more affected by statistical fluctuations than the smaller size events. To improve our statistics (e.g., to minimize fluctuations) and increase the range of values for S, τ, and Δt significantly, several alterations would be required: a much larger sprayed surface, longer measurement times, and lower flow rates. However, experimental and computer limitations prevented us from making these changes.

In summary, the general motivation of this work is twofold: The physics of continuously driven water droplet avalanches has not been systematically explored so far, and more specifically, the new paradigm of critical dynamical attractors, studied in a variety of different systems, has not yet been examined in detail for fluids. At both high and low viscosities and at low flow rates ($\sim$ 8 cm^3/min) we have found avalanche scale invariance in analogy with other nonfluid systems. Furthermore, higher viscosities provided a larger range of power law behavior due to the increased "cohesive strength" (i.e., viscosity) between the droplets. At high flow rates ($\sim$ 17 cm^3/min), the event distributions did not exhibit scale invariance, but rather decayed exponentially, implying a subcritical state with characteristic length and time scales. By lowering the input current (i.e., flow rate), the system moved from a subcritical regime to a state with no characteristic scales.

This work was supported in part by NSF Grant No. DMR-90-01502 (FN) and a Research Opportunity Award from the Research Corporation (M.B.). B.P. received support for undergraduate students from the NSF-REU.

[1] See, e.g., A.M. Cazabat, Contemp. Phys. **28**, 347 (1987); P.G. de Gennes, Rev. Mod. Phys. **57**, 827 (1985).
[2] S. Kramer and M. Marder, Phys. Rev. Lett. **68**, 205 (1992); H. Takayasu and H. Inaoka, *ibid.* **68**, 966 (1992); O. Naravan and D. Fisher (unpublished).
[3] I.M. Janosi and V.K. Horváth, Phys. Rev. A **40**, 5232 (1989).
[4] R. Shaw, *The Dripping Faucet as a Model Chaotic System* (Aerial Press, Santa Cruz, 1984); R. Cahalan *et al.*, Comput. Phys. **4**, 368 (1990), and references therein.
[5] F. Nori and S. Weiss, Michigan Report No. CM54, 1990 (unpublished); Bull. Am. Phys. Soc. **36**, 553 (1991).
[6] J.D. Scargle *et al.*, Astrophys. J. **411**, L91 (1993); J.P. Crutchfield and K. Kaneko, Phys. Rev. Lett. **60**, 2715 (1988).
[7] P.A. Bernhardt, Physica (Amsterdam) **52D**, 489 (1991); Chaos **2**, 183 (1992); S. B. Field *et al.* (unpublished).
[8] P. Bak, C. Tang, and K. Wiesenfeld, Phys. Rev. A **38**, 364 (1988).
[9] See, e.g., M. Bretz *et al.*, Phys. Rev. Lett. **69**, 2431 (1992); G.A. Held *et al.*, *ibid.* **65**, 1120 (1990); J. Rosendahl, M. Vekic, and J. Kelley, Phys. Rev. E **47**, 1401 (1993).
[10] O. Pla and F. Nori, Phys. Rev. Lett. **67**, 919 (1991).
[11] Z. Cheng, S. Redner, P. Meakin, and F. Family, Phys. Rev. A **40**, 5922 (1989); P. Meakin, Rep. Prog. Phys. **55**, 157 (1992), and references therein.
[12] T. Hwa and M. Kardar, Phys. Rev. A **45**, 7002 (1992).
[13] K.P. O'Brien and M.B. Weissman, Phys. Rev. A **46**, 4475 (1992); H.J. Jensen *et al.*, Phys. Rev. B **40**, 7425 (1989); H.J. Jensen, Phys. Rev. Lett. **64**, 3103 (1990); M.B. Weissman, Rev. Mod. Phys. **60**, 537 (1988); **65**, 829 (1993).